Seismic azimuthal impedance anisotropy in the Barnett Shale

Kui Zhang, Bo Zhang, J. Tim. Kwiatkowski, and Kurt J. Marfurt, University of Oklahoma

Summary

The Barnett Shale is one of the first and most fully developed shale gas plays in North America. In this play, the knowledge of natural and induced fracture orientation and intensity is of great importance in the choice of drilling direction and completion program. In this study, the organic-rich Barnett Shale reservoir has been extensively hydro-fractured by high pressure to simulate production prior to the acquisition of the 3D seismic survey. The objective is to recognize gas- or water- charged induced damaged rock and to identify any bypassed pay.

We migrate our seismic data using a new binning approach that sorts the data by azimuth as it is imaged in the subsurface. The motivation for this binning method is to better image lineaments as indicated by the most-positive principal curvature. We find a preferential image when structural lineaments lie perpendicular to the illumination direction. We also measure the impedance as a function of azimuth in an effort to determine the present day stress field and induced fractures in the Barnett Shale. Since velocity is anisotropic in the presence of anisotropic stress fields and/or the presence of natural or induced fractures, P-wave impedance, which is the product of density and velocity, is also anisotropic. The resultant image of the azimuth of maximum impedance and degree of impedance anisotropy correlates well with the k_1 most positive principal curvature.

Introduction

The Barnett Shale is an important unconventional shale gas system in the Fort Worth Basin, Texas where it serves as a source rock, seal, and trap. Since it has a very low permeability for production, Devon energy launched a program that fractured the rocks in the field in recent years by injecting high pressure fluid with 10 wells per square mile, thereby significantly improving the production rate. Accurately mapping the orientation and frequency of occurrence of fractures, and the stress field can significantly impact production from horizontal wells.

Seismic data offers an indirect measure of fractures and stress field though using shear wave birefringence (Alford, 1986; Crampin, 1985; Michelena, 1995), P-wave velocity variation with azimuth (Sicking et al., 2007; Roende et al., 2008; Jenner, 2001; Treadgold et al., 2008), Amplitude vs. Azimuth (AVAz) (Ruger, 1998; Luo et al., 2004; Goodway et al., 2006), and seismic attribute analysis (Chopra et al., 2007; Chopra et al., 2008).

In this study, the seismic data are migrated into different azimuth by using the new binning approach which has proven to be effective for improved illumination of faults and fractures. Next, prestack-conditioning is applied to CRP gathers to improve the signal-noise ratio. The most positive principal curvature from different azimuthal stacks behaves differently, and the structural lineaments tend to be illuminated sharper when their orientation are normal to azimuth of illumination.

Identifying and picking azimuthal variation through sinusoidal residuals in the Barnett Shale can be challenging. In order to reduce tuning effects and the effect of the seismic wavelet, we computed P-wave impedance inversion on four azimuthal stacks. Next we corrected for velocity anisotropy by snapping the full azimuth picks to the azimuth limited picks and flattening on the base horizon. Once flattened, we fit sinusoids to the four AI volumes to obtain the maximum AI direction and degree of AI anisotropy at each sample. We hypothesize that the resulting azimuthal AI anomalies are due to a combination of hydraulically-induced fluid-filled fractures and azimuthal variation in the horizontal stress.

New binning approach and data conditioning

Unlike conventional azimuthal sorting using the azimuth connecting surface sources and receivers, Perez and Marfurt (2008) proposed a new azimuth binning algorithm which takes the average path traveled from source to image point, and back to receiver (Figure 1a). The new binning method has proven to be effective for improved illumination of faults and fractures because it separates the weak side-scattering component caused by fault terminations, fractures, steep reflectors from the stronger reflections that fall within the sagittal plane. Through this azimuthal binning, seismic data are migrated into different azimuth and offset sectors as shown in Figure 1b. In our study, the data are migrated into four azimuthal bins.

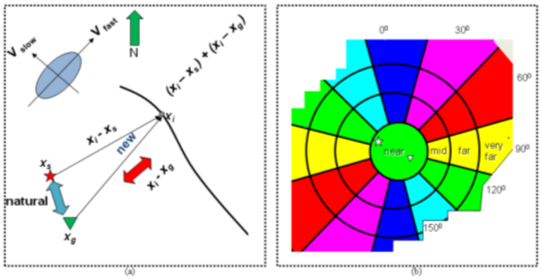

Figure 1: Diagram of new azimuthal binning (a), and the output of the migration divided into different offset and azimuth sectors (b).

Our prestack conditioning approach takes CRP gathers and raw stacks as input to form a noisy model, and then the adaptive subtraction is performed to improve the signal-to-noise ratio. Figure 2a and 2b show three gathers before- and after conditioning. Note how many events become more continuous and visible after conditioning.

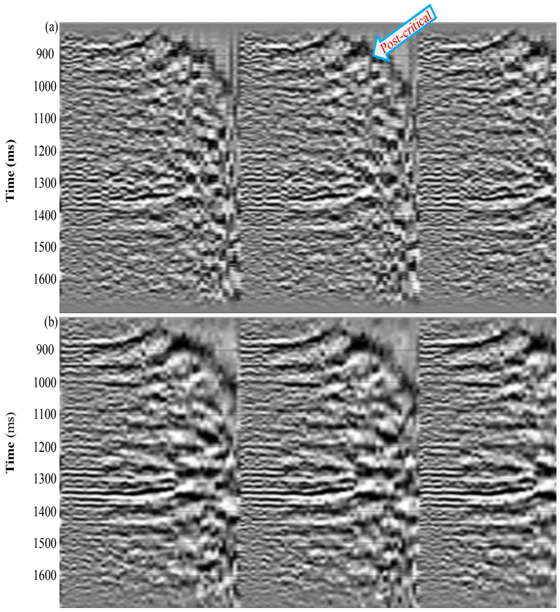

Figure 2: Raw migrated gathers (a), and the pre-stack conditioning result (b). Notice the great improvement of signal-noise ratio.

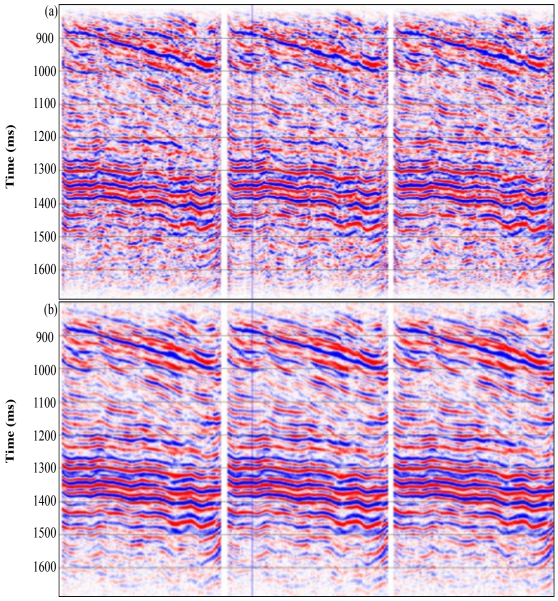

Figure 3: Migration stacks from raw migrated gathers (a), and the data-conditioning result (b).

Once the data are stacked, recursive structural oriented filtering, deconvolution, and spectral balancing are applied to further improve the image quality. Figure 3a and 3b compares three represented stacked lines before and after data preconditioning.

Figure 4 shows the most-positive principal structural curvature images corresponding to the four different azimuths. The folds, flexures, and fracture lineaments are better imaged when they are perpendicular to the seismic ray propagation direction.

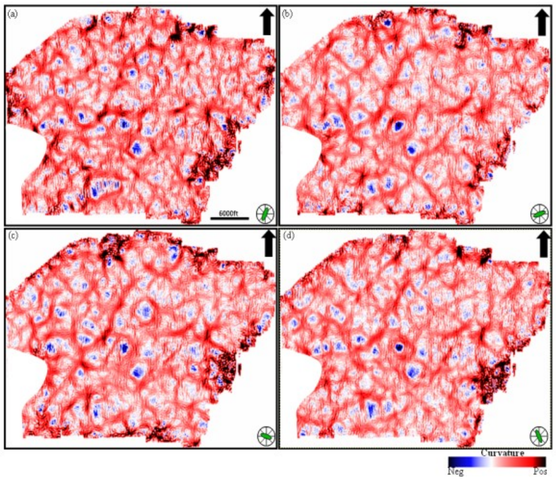

Figure 4: k_1 most positive principal curvature from azimuth 25° (a), 70° (b), 115° (c), and 150° (d). Note that lineaments are well illuminated when they are perpendicular to seismic rays.

Acoustic impedance anisotropy

The existence of fractures and anisotropic stress fields in tight reservoirs will result in the velocity variations with azimuth, and thereby the acoustic impedance (Figure 5) resulting in different reflectivity as a function of azimuth. Computing acoustic impedance as a function of azimuth removes the seismic wavelet and thin-bed tuning effects, thereby improving our anisotropy estimates of fractures and the stress field.

Before impedance inversion, we manually pick the Lower Barnett Shale in the full stacked data. Then, using this pick as the constraint, the same horizon under every azimuthal stack is picked automatically by snapping within a very small window. Figure 6 shows the picks from different stacks, where we note the small variation in time among them. Given these horizons, each of the four AI volumes are flattened and a sinusoid fit to the impedance (Figure 7) to derive the maximum and minimum AI values, anisotropy, and azimuth. During this process, the result from a good fit (7a) will be kept and the one (7b) having a high RMS error will be invalid.

Figures 8a show the maximum AI azimuth, 8b the maximum value of AI, 8c the co-rendered plot of the two, and 8d the most positive curvature from Lower Barnett Shale. We observe that there is the close spatial relationship between these figures. For example, the strongest anisotropy is correlated to strong anticlinal folds seen in the curvature map. Also, we see a clear NE trend indicated by the black arrows. Figure 9 shows the direction of maximum impedance of the small zone in red rectangle of Figure 8c based on above results, with acoustic impedance as the background color.

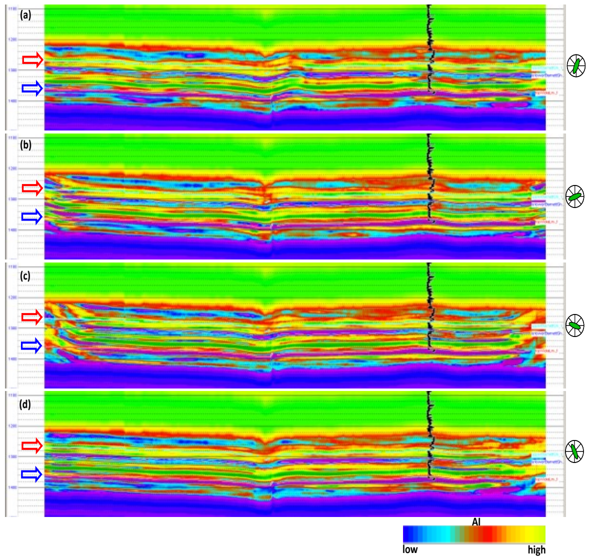

Figure 5: Acoustic impedance from different azimuth stacks. Red blocky arrows point to top Barnett Shale, and blue ones point to top Viola Limestone. Notice the AI difference from different azimuth.

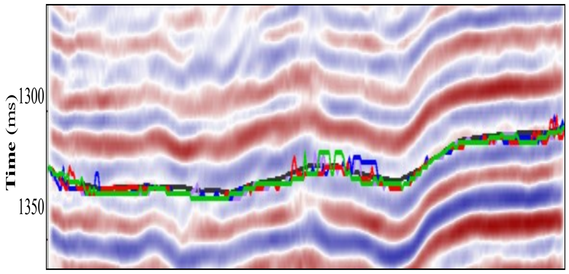

Figure 6: Lower Barnett Shale horizon picks from different azimuth data. Black, red, blue, purple, green represent manual picks, and picks from 25, 70, 115, 160 azimuthal stacks respectively.

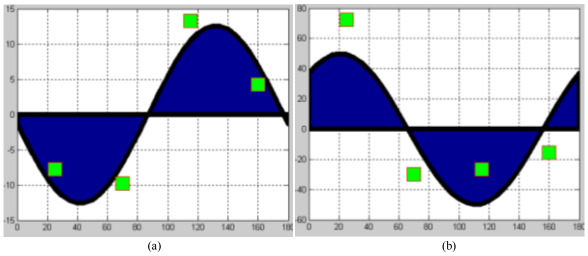

Figure 7: Example of a good sinusoidal fit (a) and bad one (b) by using four samples.

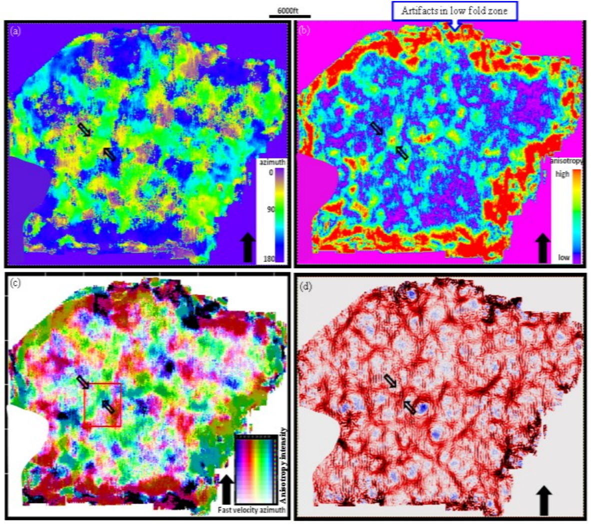

Figure 8: Fast impedance direction (a), maximum impedance (b), co-rendered plot (c) from a and b, and most positive curvature (d). Notice the correlation of them pointed by arrows.

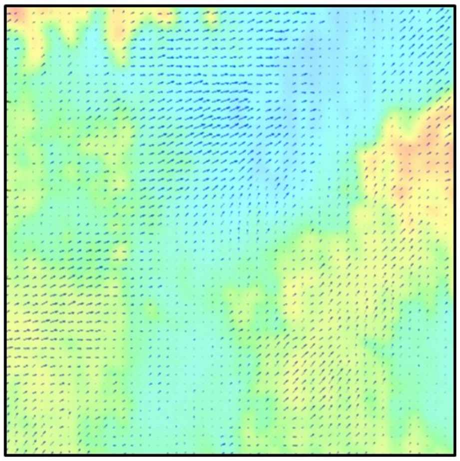

Figure 9: Vector plot of fast AI direction and anisotropy strength corresponding to the red rectangle zone in figure 8c with colored acoustic impedance at background.

Conclusions

We demonstrate that the azimuthal acoustic impedance volumes can be used as an improved means to map fractures and stress field. Furthermore, we note a close spatial relationship between the fast AI azimuth, maximum AI, and structural curvature.

We anticipate correlating these results to cores and image logs from the survey to further understand the anisotropy of the Barnett Shale. We will also extend this approach to the AVO slope and shear impedance to extensively explore its feasibility.

Acknowledgement

The authors would like to thank Devon Energy for funding, encouragement, and the authorization to publish this work. We also thank Heloise B. Lynn for her insight and technical advice.